Shock Waves (1998) 8: 11–21

Shock Waves

Gradients at a curved shock in reacting flow

H. G. Hornung

Graduate Aeronautical Laboratories, California Institute of Technology, Pasadena, California 91125, USA

Received 12 February 1997 / Accepted 10 June 1997

Abstract. The inviscid equations of motion for the flow at the downstream side of a curved shock are solved for the shock–normal derivatives. Combining them with the shock–parallel derivatives yields gradients and substantial derivatives. In general these consist of two terms, one proportional to the rate of removal of specific enthalpy by the reaction, and one proportional to the shock curvature. Results about the streamline curvature show that, for sufficiently fast exothermic reaction, no Crocco point exists. This leads to a stability argument for sinusoidally perturbed normal shocks that relates to the formation of the structure of a detonation wave. Application to the deflection–pressure map of a streamline emerging from a triple shock point leads to the conclusion that, for non–reacting flow, the curvature of the Mach stem and reflected shock must be zero at the triple point, if the incident shock is straight. The direction and magnitude of the gradient at the shock of any flow quantity may be written down using the results. The sonic line slope in reacting flow serves as an example. Extension of the results — derived in the first place for plane flow — to three dimensions is straightforward.

Key words: Streamline curvature, Crocco point, Pressure–deflection map, Mach reflection, Detonation, Shock stability, Vorticity, Sonic line

1 Introduction

Physical shock waves, which always have finite thickness, may be modeled mathematically as infinitesimally thin entities across which physical properties change discontinuously. The relation between the two states at the discontinuity is supplied by the conservation equations. Thus, given the local and instantaneous velocity of propagation of a shock relative to the medium and the orientation of this velocity relative to the tangent–plane to the shock, the local and instantaneous conditions on the downstream side of the shock may be determined from the upstream state on the shock and the thermodynamic properties of the medium. This is true even if the shock is curved and accelerating, and if it is propagating into a medium in which finite gradients exist. Such relations will be referred to in the following as the shock–jump relations.

When dealing with curved or accelerating shocks, or with non–uniform upstream media, it is sometimes useful to extend the shock–jump relations to include the connections between curvature or acceleration of the shock, and the gradients on the downstream side of the shock. The case considered here is that of a stationary curved shock with uniform upstream conditions in a steady flow of a perfect or a reacting gas. In this case the shock curvature and reaction rate determine the gradients on the downstream side of the shock.

A number of textbooks on gasdynamics partially cover this topic, *e. g.*, Hayes and Probstein (1959), Oswatitsch (1952), and several publications treat different aspects, *e. g.*, Lighthill (1949), Munk and Prim (1948), Clarke(1969), Mölder(1971). To present the problem coherently it is necessary to repeat the analyses of previous publications to some extent. In doing so the present approach begins with the analysis of Hornung (1976), in which the equations required for the present problem were used as a starting point for an asymptotic analysis of endothermic reacting flow downstream of a convex shock.

2 Definition of the problem

Consider a curved shock wave in a uniform free stream characterized by velocity V'_∞, density ρ'_∞. The origin of the shock–aligned curvilinear coordinates x', y' is chosen at the point where the streamline of interest crosses the shock wave. Let the shock curvature at this point be k' and the shock and deflection angles be β and δ as shown in Fig. 1. Introduce dimensionless variables defined by

$$h = h'/V_\infty^{'2}, \qquad p = p'/\rho'_\infty V'^2_\infty, \qquad v = v'/V'_\infty,$$
$$\rho = \rho'/\rho'_\infty, \qquad y = y'k'_0, \qquad k = k'/k'_0,$$

where h, p, ρ, v are dimensionless specific enthalpy, pressure, density and y-velocity, and k'_0 is a convenient reference value of the shock curvature. The x–component of velocity u is made dimensionless in the same way as v.

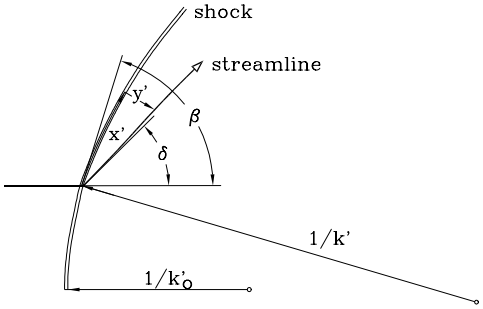

Fig. 1. Notation. Upstream of the curved shock wave, conditions are assumed to be uniform. The origin of coordinates is the point where the streamline of interest crosses the shock

The gas is supposed to obey caloric and thermal equations of state of the forms

$$h = h(p, \rho, c_i), \tag{1}$$

$$T = T(p, \rho, c_i), \tag{2}$$

in which T is the dimensionless absolute temperature $RT'/V_\infty'^2$, with the specific gas constant R, and the c_i are the mass fractions of the n constituent species of the gas, i taking values 1 through n.

Since the mass fractions must satisfy the identity

$$\sum_{i=1}^{n} c_i = 1 \ ,$$

the number of mass fractions that are independent is one less than the total number n of components present. It is usually convenient to choose c_1 as a dependent variable and the other c_i's as independent variables. Thus,

$$dh = h_\rho d\rho + h_p dp + \sum_{i=2}^{n} h_{c_i} dc_i$$

where the subscripts denote partial differentiation.

In order to determine the gradients of physical properties of the flow at the shock wave, it is necessary to solve the differential equations of motion for the components of the gradients. To do this, consider the two components of the inviscid momentum equations, the y–differentiated energy equation and the continuity equation as follows:

$$uu_x + (1-ky)vu_y - kuv + p_x/\rho = 0, \tag{3}$$

$$uv_x + (1-ky)vv_y + ku^2 + (1-ky)p_y/\rho = 0, \tag{4}$$

$$h_p p_y + h_\rho \rho_y + \sum_{i=2}^{n} h_{c_i} c_{iy} + vv_y + uu_y = 0, \tag{5}$$

$$(\rho u)_x - k\rho v + (1-ky)(\rho v)_y = 0. \tag{6}$$

The case of interest here is $y = 0$, *i. e.*, the term $(1 - ky)$ that occurs in these equations may be written as 1 for our purposes. The x–differentiated form of the energy equation

$$\rho_x = -(uu_x + vv_x + h_p p_x)/h_\rho, \tag{7}$$

will also be needed, as will the shock–jump relations

$$p - p_\infty = \sin^2\beta\left(1 - 1/\rho\right), \tag{8}$$

$$c_i = c_{i\infty}, \tag{9}$$

$$v = \sin\beta/\rho, \tag{10}$$

$$2(h - h_\infty) = \sin^2\beta\left(1 - 1/\rho^2\right), \tag{11}$$

$$u = \cos\beta, \tag{12}$$

$$\rho = \frac{\gamma + 1}{\gamma - 1 + 2/(M^2\sin^2\beta)}, \tag{13}$$

where γ is the ratio of specific heats, and M is the free–stream Mach number. The expression for the density ratio across the shock, Eq. (13), is written for a constant–γ gas. This is permissible in a reacting flow situation if the shock–jump relations are taken to apply to the jump from the free–stream conditions to the conditions downstream of the shock before any reactions take place, *i. e.*, to a jump that does not involve a change of composition, as is made clear by Eq. (9).

The problem of determining the gradients of the flow variables at the shock consists of solving Eqs. (3 to 6) for the y–derivatives, and determining the x–derivatives (along the shock) by differentiating the shock–jump relations with respect to x.

So far it has been tacitly assumed that the flow is plane. As will be seen later, the extension to the general case is quite straightforward.

3 Partial and substantial derivatives at the shock

Differentiation of the shock–jump conditions with respect to x introduces the shock curvature $\beta_x = -k$:

$$\frac{u_x}{k} = \sin\beta \tag{14}$$

$$\frac{\rho_x}{k} = -\frac{4\rho^2\cos\beta}{(\gamma+1)M^2\sin^3\beta} \tag{15}$$

$$\frac{p_x}{k} = -2\sin\beta\cos\beta\left(1 - \frac{1}{\rho}\right) + \frac{\sin^2\beta}{\rho^2}\frac{\rho_x}{k} \tag{16}$$

$$\frac{v_x}{k} = -\frac{\cos\beta}{\rho} - \frac{\sin\beta}{\rho^2}\frac{\rho_x}{k}. \tag{17}$$

Solving Eqs. (3 to 6) for the y–derivatives yields:

$$p_y F = \rho\sum_{i=2}^{n} h_{c_i} c_{iy} - k\rho\left[u\left(1 - \frac{\rho h_\rho}{v^2}\right)K + \frac{u}{v}E + \rho\frac{h_\rho}{v}L\right] \tag{18}$$

$$u_y = -\frac{kE}{v} \tag{19}$$

$$vv_y F = -\sum_{i=2}^{n} h_{c_i} c_{iy} + k\left[\rho u h_p K + \frac{u}{v}E + \rho\frac{h_\rho}{v}L\right] \tag{20}$$

$$\rho_y F = \frac{\rho}{v^2}\sum_{i=2}^{n} h_{c_i} c_{iy} - \frac{k\rho}{v^2}\left[\rho u h_p K + \frac{u}{v}E + (1 - \rho h_p)L\right], \tag{21}$$

where

$$K = \frac{v_x}{k} + u, \tag{22}$$

$$L = \frac{(\rho u)_x}{\rho k} - v, \tag{23}$$

$$E = \frac{p_x}{\rho k} + u\frac{u_x}{k} - uv, \tag{24}$$

$$F = 1 - \rho\left(\frac{h_\rho}{v^2} + h_p\right). \tag{25}$$

The y-derivatives of the c_i have to be kept as components of a parameter, because they depend on the reaction rates, which are functions of state that have so far been left unspecified. As may be seen from Eqs. (14 to 17), any x–derivative is proportional to k, so that ratios like p_x/k are independent of the shock curvature, and all such ratios are known on the shock in terms of the free–stream conditions and β.

With both x– and y–derivatives known, it is now possible to form substantial derivatives according to

$$\frac{d}{dt} = u\frac{\partial}{\partial x} + v\frac{\partial}{\partial y}. \tag{26}$$

For example, noting that the deflection angle is

$$\delta = \beta - \arctan(v/u), \tag{27}$$

forming the derivatives of this function with respect to x and y, and writing

$$V = ds/dt = \sqrt{v^2 + u^2}, \tag{28}$$

where s is distance along the streamline measured from the origin, the streamline curvature at the shock, $d\delta/ds$ is obtained as

$$\frac{vV^3}{u}F\frac{d\delta}{ds} = \sum_{i=2}^{n} h_{c_i}\frac{dc_i}{dt} + \frac{k}{v}\left(\rho h_\rho G - \frac{vV^2}{\rho u}\frac{p_x}{k}F\right), \tag{29}$$

where

$$G = V^2 + \frac{uv_x}{k} - \frac{up_x}{\rho v k} - v\frac{u_x}{k}. \tag{30}$$

Similarly, other substantial derivatives may be formed:

$$F\frac{dp}{dt} = \rho\sum_{i=2}^{n} h_{c_i}\frac{dc_i}{dt} + kG\frac{\rho^2 h_\rho}{v}, \tag{31}$$

$$F\frac{d\rho}{dt} = \frac{\rho}{v^2}\sum_{i=2}^{n} h_{c_i}\frac{dc_i}{dt} - kG\frac{\rho^2}{v}\left(h_p - \frac{1}{\rho}\right), \tag{32}$$

$$V\frac{dV}{dt} = -\frac{1}{\rho}\frac{dp}{dt}. \tag{33}$$

At this point it is worth taking a closer look at these results. Note that the streamline curvature and the substantial time–derivatives all consist of two terms, one of which is proportional to the rate of change of specific enthalpy of the gas that is caused by chemical reaction, and the other is proportional to the shock curvature. (It is important to remember that the coefficients of these two parameters – reaction rate and shock curvature – are all determined by the free–stream conditions and the shock–jump relations). It follows that, for non–reacting flow, all of these derivatives are proportional to the shock curvature, through a proportionality factor that depends on the free–stream conditions and the shock angle. Conversely, for chemically reacting flow through a straight shock, the streamline curvature and time derivatives are directly proportional to the rate of specific enthalpy removal by chemistry.

A special case of some interest warrants discussion: In inviscid chemically reacting flow over a plane wedge at an angle sufficiently small to give an attached shock, the streamline curvature at the tip of the wedge has to be zero (plane wedge) and Eq. (29) gives

$$\sum_{i=2}^{n} h_{c_i}\frac{dc_i}{dt} = -\frac{k}{v}\left(\rho h_\rho G - \frac{vV^2}{\rho u}\frac{p_x}{k}F\right), \tag{34}$$

i. e., the reaction–rate parameter is proportional to the shock curvature at the tip, as has been pointed out by Clarke (1969), Becker (1972) and others. This has also been used to determine reaction rates experimentally by Smith and Wegener (see Becker, 1972) and by Kewley and Hornung (1974).

Another interesting observation may be made by forming the ratio of Eqs. (31) and (32). This gives

$$\frac{dp}{d\rho} = v^2\frac{\sum_{i=2}^{n} h_{c_i}dc_i/dt + kG\rho h_\rho/v}{\sum_{i=2}^{n} h_{c_i}dc_i/dt - kG\rho v\left(h_p - 1/\rho\right)}. \tag{35}$$

Both the numerator and the denominator obviously contain two terms, one from shock curvature and one from reaction rate. Again consider the limiting cases of non–reacting flow and straight shock: In the case of non–reacting flow, the first terms in the numerator and in the denominator vanish. This has the interesting consequence that the curvature terms also cancel, so that the derivative of p with respect to ρ along the streamline also becomes independent of the shock curvature! The equation reduces to

$$\frac{dp}{d\rho} = -\frac{h_\rho}{h_p - 1/\rho}. \tag{36}$$

This is just the expression for the value of this derivative at constant entropy (the square of the frozen speed of sound) for a gas with a general caloric equation of state. This is as it should be, since the entropy will be constant along a streamline in non–reacting flow.

In the other limit, that of reacting flow through a plane shock, omitting the curvature terms again causes the other parameter to cancel as well, and gives the well–known result

$$\frac{dp}{d\rho} = v^2. \tag{37}$$

4 Streamline curvature

Many interesting features of flows may be understood better by studying the streamline curvature at a shock. This is, of course, only one case where the results of the previous section about gradients at the shock can be used to advantage. However, it serves the purpose of demonstrating how the jump conditions may be extended by considering gradients.

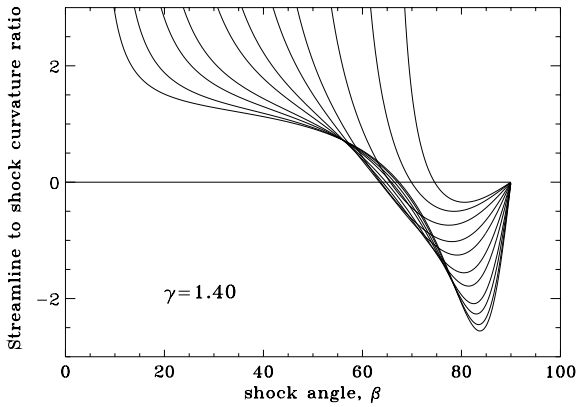

Fig. 2. Ratio of streamline to shock curvature for perfect–gas flows with γ = 1.4 and for free–stream Mach numbers 1.1 (uppermost curve), 1.2, 1.4, 1.7, 2.0, 2.5, 3,4, 5, 7, 10, 20. The ratio becomes singular at the Mach angle, and goes to zero at the normal–shock point. A zero crossing occurs again at the Crocco point (zero crossing) which always occurs between the sonic and maximum–deflection point

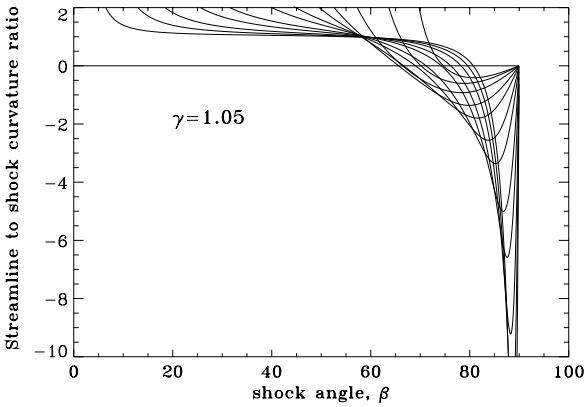

Fig. 3. Ratio of streamline to shock curvature for perfect–gas flows with γ = 1.05 and for free–stream Mach numbers 1.1, 1.2, 1.4, 1.7, 2.0, 2.5, 3, 4, 5, 7, 10, 20. Note how the high–Mach–number cases hug the ratio 1. This is close to the Newtonian limit, where the streamlines lie close to the shock for a large range of shock angles

4.1 Perfect–gas flows

With non–reacting flow, G, F, E, K, and L reduce to relatively simple functions of M, γ and β:

$$G = \left[3\cos^2\beta - \frac{\sin^2\beta}{\rho^2}\right]\left(1-\frac{1}{\rho}\right) + \frac{8\cot^2\beta}{(\gamma+1)M^2}, \quad (38)$$

$$F = -\frac{1}{\gamma-1}\left(1-\frac{\gamma p\rho}{\sin^2\beta}\right), \quad (39)$$

$$E = -\frac{\cos\beta\sin\beta}{\rho}\left[\left(3-\frac{1}{\rho}\right) + \frac{4}{\rho(\gamma+1)M^2\sin^2\beta}\right], \quad (40)$$

$$K = \cos\beta\left[1-\frac{1}{\rho} + \frac{4}{(\gamma+1)M^2\sin^2\beta}\right], \quad (41)$$

$$L = \sin\beta\left(1-\frac{1}{\rho}\right) - \frac{4\rho\cos^2\beta}{(\gamma+1)M^2\sin^3\beta}. \quad (42)$$

Evaluating the ratio of streamline to shock curvature gives the result shown in Fig. 2 for γ = 1.4. The features of the streamline–to–shock curvature ratio may be described in terms of a convex shock such as is shown in Fig. 1. At the normal–shock point the streamline curvature has to be zero, of course. It is of opposite sign to that of the shock at values of β smaller than and close to 90°, but reaches a minimum before increasing again to positive values, and finally becomes singular at the Mach angle. The zero–crossing occurs at the so–called Crocco point, at which the streamline curvature is zero for all values of the shock curvature. For perfect–gas flows, the Crocco point always lies between the point where the Mach number at the shock is unity – the sonic point – and the maximum–deflection point. Thus, for the convex shock, the streamline curvature is concave–up near the normal–shock point, and goes to convex–up at small shock angles. The singularity at the Mach angle does not mean that the streamline curvature becomes infinite, but rather that the shock curvature is identically zero there.

The dependence of the streamline to shock curvature ratio on γ may be illustrated by plotting the same graphs for γ = 1.05, see Fig. 3. At low Mach numbers the curves behave in much the same manner as for higher γ, but at higher Mach numbers the minimum is much lower, the Crocco point is pushed closer to the normal–shock point, and, as the Mach number becomes very high, the curvature ratio hugs the value 1 more and more closely and for a larger range of shock angles. This is the behavior expected as conditions approach the Newtonian limit ($M\to\infty, \quad \gamma\to 1$), where streamline and shock become almost congruent, since the density ratio across the shock approaches infinity.

4.2 Reacting flow

In order to calculate explicit values of gradients in the case of reacting flow, it is necessary to introduce a model for the caloric equation of state and for the reaction rate. For this purpose, the rate equation is written in the simple form

$$\sum_{i=2}^{n} h_{c_i}\frac{dc_i}{dt} = \frac{\theta}{\varepsilon}\exp(-\theta\rho/p), \quad (43)$$

so that a representative variation of the dependence of reaction rate on shock angle is maintained by using the Arrhenius form. The differential form of the caloric equation of state becomes

$$dh = -\frac{\gamma}{\gamma-1}\frac{p}{\rho^2}d\rho + \frac{\gamma}{\gamma-1}\frac{1}{\rho}dp + \frac{\theta}{\varepsilon}\exp(-\theta\rho/p)dt. \quad (44)$$

With this form of the reaction rate, the streamline curvature may be calculated explicitly for given values of θ and ε. the result of such a computation is plotted in Fig. 4. With the sign convention chosen in Eqs. (43) and (44), positive values of θ and ε mean that the reaction is endothermic. Thus, Fig. 4 shows the remarkable fact that, for a given set of parameters M, γ, and θ, there exists a particular reaction rate parameter ε, below which the streamline–to–shock curvature ratio is positive for all shock angles, and no Crocco point exists. The reaction rate at this point is always exothermic, *i. e.*, ε is negative at this point. For the parameters chosen in Fig. 4, the special value of ε is approximately -1/119.

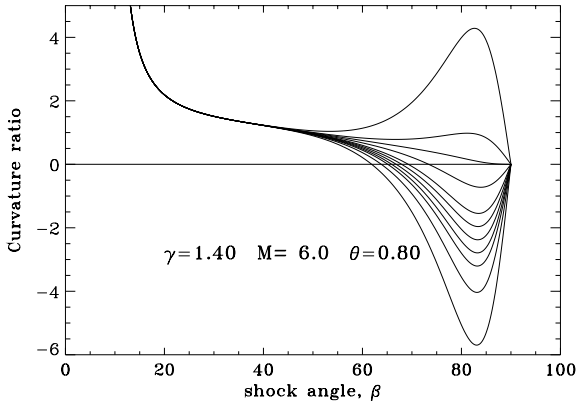

Fig. 4. Streamline to shock curvature ratio in reacting flow for γ = 1.4, M = 6 and θ = 0.8. The values of the reaction rate parameter are $1/\varepsilon$ = 160 (lowest curve), 80, 40, 20, 0.1, -20, -40, -80, -119, -160, -320

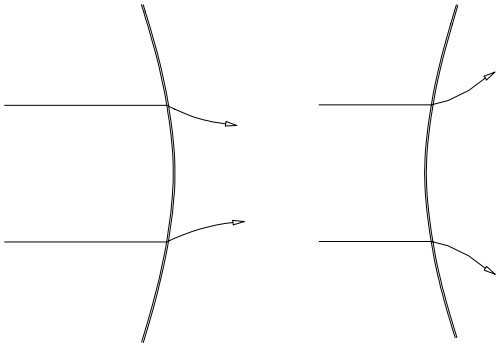

Fig. 5. Schematic sketch of a convex and concave near–normal shocks with associated streamlines, for a perfect gas. Both the concave and the convex shocks produce streamline curvatures that can exist stably in steady flow

4.3 Application to geometrically perturbed normal shock

The fact that the curvature ratio is positive near the normal–shock point, if the rate of an exothermic reaction is sufficiently fast, has interesting consequences. In order to understand this, consider first the case of a sinusoidally perturbed normal shock in a perfect gas. Figures 2 and 3 show that, for small negative perturbations of the shock angle from 90°, the streamline–to–shock curvature ratio is negative for a perfect gas. Similarly, for positive perturbations of β from 90°, the ratio will be positive. Consequently, a concave–upstream shock, which is associated with streamline convergence toward the symmetry plane of the shock, will cause the streamline curvature to be such that streamlines merge into the direction of the symmetry plane, see Fig. 5, left. A convex–upstream shock, for which the deflection is away from the symmetry plane, produces streamlines that bend away from the symmetry plane, see Fig. 5, right. This is very different in the case of a sufficiently fast exothermic reaction, of the type where no Crocco point exists, or where the streamline–to–shock curvature ratio is positive in the range $0 < \beta < 90°$. In that case, the situation is as illustrated in Fig. 6. The convex–upstream shock with deflection away from the symmetry plane is also associated with a streamline curvature away from the symmetry plane, see Fig. 6, left. On the other hand, the concave–upstream shock, with deflections

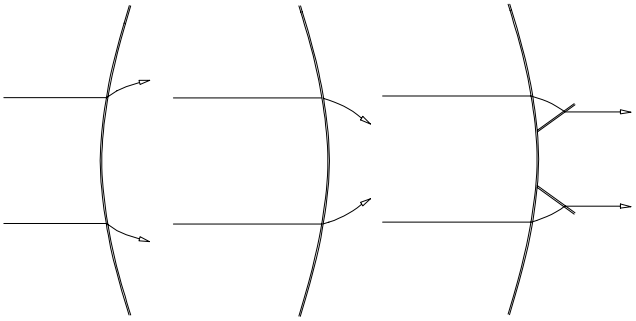

Fig. 6. Schematic sketch of a convex and concave near–normal shocks with associated streamlines, for a gas with fast exothermic reaction rate. The convex–upstream shock on the left can exist with stable steady flow. However, the concave–upstream shock shown in the center requires a pair of unsteady shocks to deflect the flow parallel to the symmetry plane (right)

toward the symmetry plane, also produces a streamline curvature toward the symmetry plane. On the symmetry plane, this causes a clash between the two convergent streamlines that will necessarily result in the production of two unsteady shock waves traveling outward from the symmetry plane, see Fig. 6, right.

Thus, it is evident that a concave–upstream shock can not give a steady solution if an exothermic reaction of sufficiently fast rate occurs at the shock. This is clearly related to the unsteady waves that occur in detonations and that form the cellular structure observed in such waves.

5 Shock and streamline in the $V\delta$–plane

Many gasdynamical problems are simplified by mapping the flow into the hodograph or uv–plane. It is sometimes more convenient to choose other variables for this mapping, such as the $V\delta$–plane, or the $p\delta$–plane. The condition after a straight shock in non–reacting flow maps into the $V\delta$ shock locus shown in Fig. 7 as the continuous curve, starting at the infinitesimally weak shock point (1,0), moving smoothly through the maximum–deflection point and back to δ = 0 at the normal–shock point. This curve is the same for flows with finite reaction rate, of course, since it just represents the shock–jump conditions, which we have taken to be the same, by choosing the composition to be unchanged across the shock.

The additional information that is brought into this picture by knowing the gradients at the shock, is that it permits curved and reacting shocks to be treated in this way as well. It is therefore convenient to treat perfect–gas and reacting flows separately.

In particular, the derivative $d\delta/dV$ may be formed by using the general results for the gradients at the shock. Thus,

$$\frac{d\delta}{dV} = \frac{d\delta}{ds}\frac{ds}{dV} = \frac{d\delta}{ds}\frac{ds}{dt}\frac{dt}{dV} = \frac{d\delta}{ds}(-\rho V^2)\frac{dt}{dp}. \tag{45}$$

Substituting from Eqs. (29) and (31), this gives

$$\frac{d\delta}{dV} = -\frac{u}{Vv}\frac{\sum_{i=2}^{n} h_{c_i}\frac{dc_i}{dt} + \frac{k}{v}\left(\rho h_\rho G - \frac{vV^2}{\rho u}\frac{p_x}{k}F\right)}{\sum_{i=2}^{n} h_{c_i}\frac{dc_i}{dt} + kG\frac{\rho h_\rho}{v}} \tag{46}$$

This derivative indicates the direction in which the streamline departs from the shock in the $V\delta$–plane.

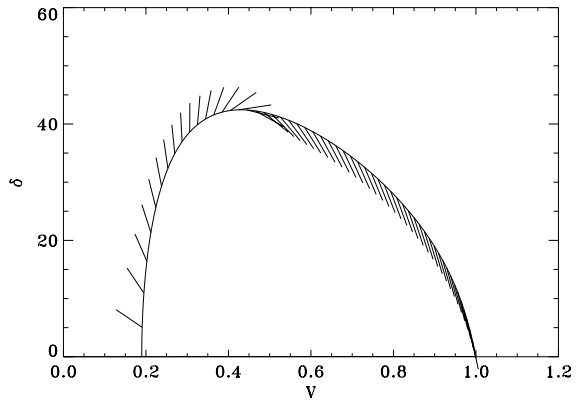

Fig. 7. $V\delta$–plane map of a curved shock in non–reacting flow with M = 6 and γ = 1.4. The short straight lines indicate the direction in which the streamline leaves the shock in the case of a convex–upstream shock. Note how the direction is parallel to the shock locus at the weak–shock point, becomes horizontal at the Crocco point, then vertical at the zero–G point, and finally horizontal again at the normal–shock point

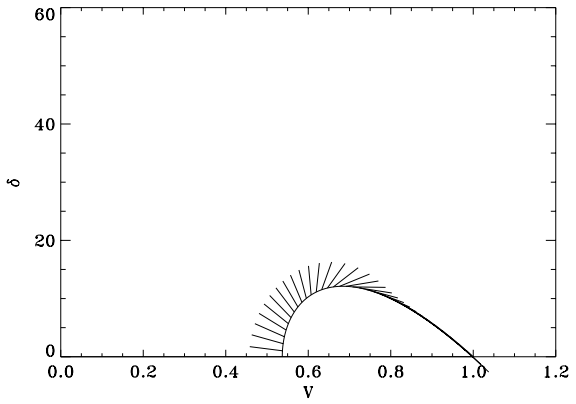

Fig. 8. For M = 1.5, γ = 1.4, the streamline direction at the convex–upstream shock is everywhere outward from the shock locus

5.1 Perfect–gas flows

For the special case of non–reacting flow, the streamline slope in the $V\delta$–plane becomes

$$\frac{d\delta}{dV} = \frac{-u}{Vv}\left[1 - \frac{vV^2}{\rho^2 h_\rho u}\frac{p_x}{k}\frac{F}{G}\right]. \tag{47}$$

In Fig. 7 this direction is indicated by a short straight line starting at the shock locus. Although the *slope* of the streamline in the $V\delta$–plane is independent of the shock curvature, its *direction* is opposite to the one shown, for a shock wave curvature of opposite sign. The direction of the streamline shown in Fig. 7 is that for a convex–upstream shock.

The streamline direction in the $V\delta$–plane undergoes several changes as we proceed from the weak–shock point to the normal–shock point. At the former, the streamline direction is parallel to the shock locus. No dramatic change occurs up to the vicinity of the Crocco point. In that vicinity, the slope changes rapidly from negative to zero at the Crocco point, and subsequently to infinite, where it changes sign to minus infinity, and then approaches zero from below at the normal–shock point. For non–reacting flow, the point at which the slope becomes infinite is easily identified as the zero–G point, see Eq. (47).

This kind of diagram was used extensively by Guderley in the hodograph plane. He called it the hedgehog or porcupine diagram. Figure 7 is a funny–looking porcupine, with some of the "spines" pointing inward. However, it becomes obvious why the term porcupine seemed appropriate to Guderley, when it is remembered that he was concerned particularly with flows in the vicinity of M = 1. Thus, Fig. 8 shows the same plot for the case M = 1.5 in which all the spines are seen to point outward.

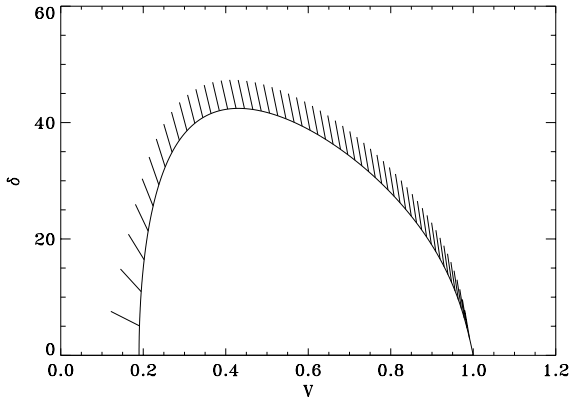

Fig. 9. Plane shock with endothermic chemical reaction. M = 6, γ = 1.4. Note the difference between the streamline slopes of this diagram and those of Fig. 7

5.2 Reacting flow

In the other extreme case of a straight shock with finite chemical reaction rate the streamline slope in the $V\delta$–plane becomes particularly simple:

$$\frac{d\delta}{dV} = -\frac{u}{Vv}. \tag{48}$$

It is clear that this slope is negative throughout the range $0 < \beta < 90$, and the spines point outward for an endothermic reaction and inward for exothermic reaction. Figure 9 shows that case with M = 6 and γ = 1.4 for endothermic reaction.

The streamline slopes in Figs. 7 and 9 are very different, especially in the weak and medium shock strength regime. Both are extreme cases, of course, and the general case of finite reaction, Eq. (46), will give slopes anywhere between the two extremes depending on the relative importance of chemical reaction and shock curvature. It is also possible to obtain the asymptotic behaviors of Eq. (46), both in the fast and slow reaction limits. To do this, introduce the parameter

$$\omega = -\frac{v\sum_{i=2}^{n} h_{c_i}\frac{dc_i}{dt}}{k\rho h_\rho} = \sin\beta\frac{\gamma-1}{\gamma}\frac{\theta}{\varepsilon k}\exp(-\theta\rho/p), \tag{49}$$

where the last expression applies for the gas model of Eq. (43). This variable measures the relative importance of reaction rate and shock curvature. It is positive for endothermic reaction and convex–upstream shocks. With this definition of ω, Eq. (46) becomes

$$\frac{d\delta}{dV} = -\frac{u}{Vv}\frac{\omega - G + \frac{vV^2}{\rho^2 h_\rho u}\frac{p_x}{k}F}{\omega - G}. \tag{50}$$

Expanding this for $\omega \to 0$, the slope becomes

$$\left(\frac{d\delta}{dV}\right)_{\omega\to 0} = -\frac{u}{Vv}\left[1 - \left(\frac{vV^2}{\rho^2 h_\rho u}\frac{p_x}{k}F\right)\frac{1}{G}\left(1+\frac{\omega}{G}\right)\right] + \mathrm{O}(\omega^2). \tag{51}$$

In the other limit, we obtain

$$\left(\frac{d\delta}{dV}\right)_{\omega\to\infty} = -\frac{u}{Vv}\left[1 + \frac{1}{\omega}\left(\frac{vV^2}{\rho^2 h_\rho u}\frac{p_x}{k}F\right)\right] + \mathrm{O}\left(\frac{1}{\omega^2}\right). \tag{52}$$

It is opportune here to stress again that the functions on the right of 50 to 52 may all be expressed in terms of the free–stream conditions, β and ω.

The manner in which $d\delta/dV$ changes with reaction rate is shown for M = 6, γ = 1.4 and θ = 0.8 in Fig. 10, using the reaction rate model of Eqs. (43) and (44). Consider first the full lines in this graph: In the weak–shock limit, the slope has a finite negative value. For a given value of $k\varepsilon$, as β is increased from the weak–shock limit, the slope increases and becomes infinite at a particular value of β, then rises from negative infinity, toward zero at the normal–shock point. This rise occurs almost exactly along the straight–shock curve, which is the lower convergence line in the graph. Note that, for straight shocks, *i. e.*, infinite ω the slope is negative everywhere except at the normal–shock point, independently of whether ω is positive or negative. This is the reason why this line is a convergence line between the dashed and full curves. In the $V\delta$–plane the difference between endothermic and exothermic reactions would be that the streamlines would leave the shock (at the same slope) in opposite directions. The upper convergence line is the value for a curved shock in non–reacting flow, the curve labeled $k\varepsilon = \pm 1$.

It is interesting to consider a particular shock angle, say 55° and fixed shock curvature, and changing ε from ∞ (non–reacting flow) to 0 (fast reaction rate). The slope starts on the upper convergence line ($k\varepsilon = \pm 1$), where $d\delta/dV$ is approximately –1.8, then increases rapidly to ∞ at $\varepsilon \simeq 10^{-3}$, where it flips to $-\infty$ and then approaches the lower convergence line from below. For a convex–upstream shock, these changes represent a smooth anticlockwise rotation of the "spine" of the porcupine from the direction in Fig. 7 to that in Fig. 9.

6 Three–shock points

Across the streamline coming out of an intersection of three shock waves in inviscid, steady flow the velocity is discontinuous, but the deflection and pressure are continuous. This

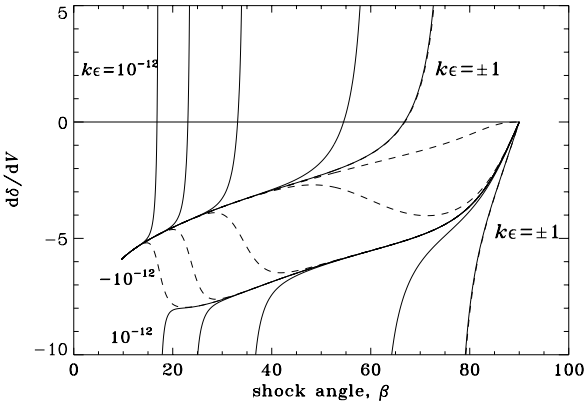

Fig. 10. Effect of reaction rate on $d\delta/dV$ as a function of shock angle, for M = 6, γ = 1.4 and θ = 0.8. The values of the reaction rate parameter are $k\varepsilon$ = 1, 10^{-3}, 10^{-6}, 10^{-9}, 10^{-12}, –1, –0.0084, -10^{-3}, -10^{-6}, -10^{-9}, and -10^{-12}. The dashed lines indicate the cases where the reaction is exothermic. The lower convergence line corresponds to the straight–shock solution shown in Fig. 9. The non–reacting curved–shock case is the upper convergence line at low shock angles, and – at larger shock angles – may be identified as the lines for $k\varepsilon = \pm 1$ that are practically congruent

makes representation of the flow in the δp–plane very attractive. With the knowledge of the gradients, it is relatively simple to extend arguments about triple points of straight shocks to include cases where the shocks are curved. To this end, the derivative $d\delta/dp$ at a curved shock may be evaluated quite straightforwardly as:

$$\frac{d\delta}{dp} = \frac{d\delta}{ds}\frac{ds}{dp} = \frac{d\delta}{ds}\frac{ds}{dt}\frac{dt}{dp} = \frac{d\delta}{ds}V\frac{dt}{dp}. \tag{53}$$

Substituting from Eqs. (29) and (31),

$$\frac{d\delta}{dp} = \frac{u}{\rho V^2 v}\frac{\sum_{i=2}^{n} h_{c_i}\frac{dc_i}{dt} + \frac{k}{v}\left(\rho h_\rho G - \frac{vV^2}{\rho u}\frac{p_x}{k}F\right)}{\sum_{i=2}^{n} h_{c_i}\frac{dc_i}{dt} + kG\frac{\rho h_\rho}{v}}, \tag{54}$$

which is just $(-1/\rho V)d\delta/dV$. This means that the qualitative behavior of $d\delta/dp$ is like $-d\delta/dV$.

An example of the occurrence of a triple point is the Mach reflection of a straight shock from a wall, as shown schematically in the upper part of Fig. 11. The lower part of Fig. 11 shows a map of non–reacting flow of this kind in the δp–plane. The regions labeled 1 through 5 in the physical space are labeled similarly at the corresponding points in the δp–space. Now suppose that, at the triple point, the Mach stem is curved, the incident shock is plane, and the reflected shock is curved. Since δ and p must be continuous across the slip line not only at the triple point, but also at ds from the triple point, $d\delta/dp$ has to be continuous across the slip line at the triple point.

The value of $d\delta/dp$, for non–reacting flow and a concave–upstream shock, gives the slopes and directions shown in Fig. 11 for the chosen parameters. It is clear from Fig. 11 that, with a straight incident shock, the slope in δp–space of the slip line issuing from the Mach stem is *not* the same as that issuing from the reflected shock at the point 3,4. Since the slopes are independent of the shock curvatures, there is no possibility for the curvatures to adjust to meet the constraint. The only possible conclusion to be drawn from

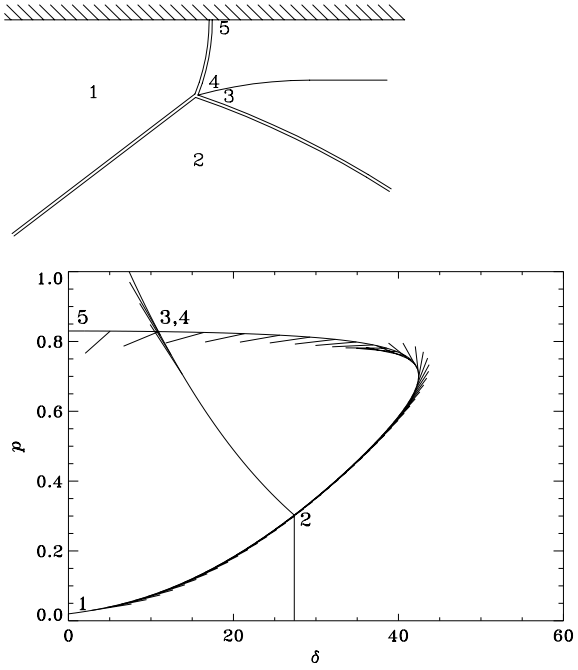

Fig. 11. Mach reflection. Top: Schematic sketch of the shock configuration, with labels identifying regions and points of the flow in physical space. Bottom: δp–map of this flow, showing the incident shock (1–2), the reflected shock (2–3) and the Mach stem (4–5), as determined from the shock–jump relations. M = 6, γ = 1.4, non–reacting steady flow. Also shown are the streamline directions from the reflected shock and the Mach stem. Note that the two streamline directions coming from 3 and 4 are not the same, leading to the conclusion that these two shocks must have zero curvature at the triple point

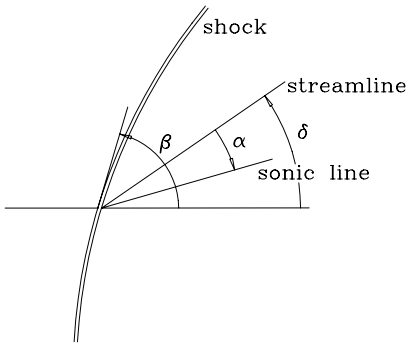

Fig. 12. Definition of angles

this result is that – in non–reacting flow – the curvatures of both the Mach stem and the reflected shock must be zero at the triple point (except in very special cases). This is not to say that these two shocks can not be curved at other locations, but rather that – at the triple point – both have a point of inflection. (In the more general case of a curved incident shock, Mölder (1972) shows that the curvature of the other shocks need not be zero.)

It is interesting that this result may be different for the case of reacting flow. This is because, with finite reaction rate, $d\delta/dp$ is no longer independent of the shock curvature. The reaction therefore provides an additional degree of freedom that may permit the shocks to assume the finite curvatures that correspond to the local reaction rates and the streamline curvature constraint at the triple point.

7 Some other derivatives

The derivatives of the flow quantities at the shock obtained in Sect. 3 permit a number of other interesting quantities to be determined. In this section the vorticity at a shock is used as an example, and an illustration of how the results may be used generally is given.

7.1 Vorticity at the shock

In the curvilinear coordinates chosen, the vorticity at the shock is given by

$$\zeta \;=\; u_y \;-\; v_x \;+\; ku. \tag{55}$$

Substituting for u_y from Eqs. (19) and (24), this becomes

$$\zeta \;=\; -\frac{k}{v}\left(\frac{p_x}{\rho k} \;+\; u\frac{u_x}{k} \;-\; uv \;-\; v\frac{v_x}{k} \;+\; uv\right). \tag{56}$$

In this expression, the terms with explicit Mach–number and γ dependence in the $p-$ and $v-$derivative terms cancel when using Eqs. (8–17), and only the $\beta-$ and $\rho-$dependence remains. The result is

$$\zeta \;=\; -k\rho\cos\beta\left(1 \;-\; \frac{1}{\rho}\right)^2. \tag{57}$$

This is the well–known expression for the vorticity at a curved shock, see *e. g.*, Hayes and Probstein (1959). Clearly, the vorticity *at the shock* is independent of the reaction rate. Note that this is because the problem considered here is that where the composition is constant across the shock and contributions from the reaction occur only after the shock, rather than that of equilibrium shocks.

7.2 Gradients at the shock, sonic line direction

The results of Sect. 3 may be used to determine the magnitude and direction of the gradient of any flow quantity. For example, the pressure gradient direction and magnitude will be

$$\arctan(p_y/p_x), \qquad \sqrt{p_y^2 + p_x^2}. \tag{58}$$

Since reactions strongly affect the direction of the density gradient, knowledge of this direction is very valuable, for example, in the interpretation of interferograms of reacting flow. Other gradients are of interest. For example, the slope of the sonic line, for which a closed–form solution exists in the case of plane flow of a perfect gas (see Hayes and Probstein, 1959), is also affected by the reaction rate.

In order to determine the sonic line slope, consider the energy equation for our isoenergetic flow and the model gas in the form

$$\frac{V^2}{2} \;+\; \frac{a^2}{\gamma - 1} \;+\; h_{\text{chem.}} \;=\; h_0, \tag{59}$$

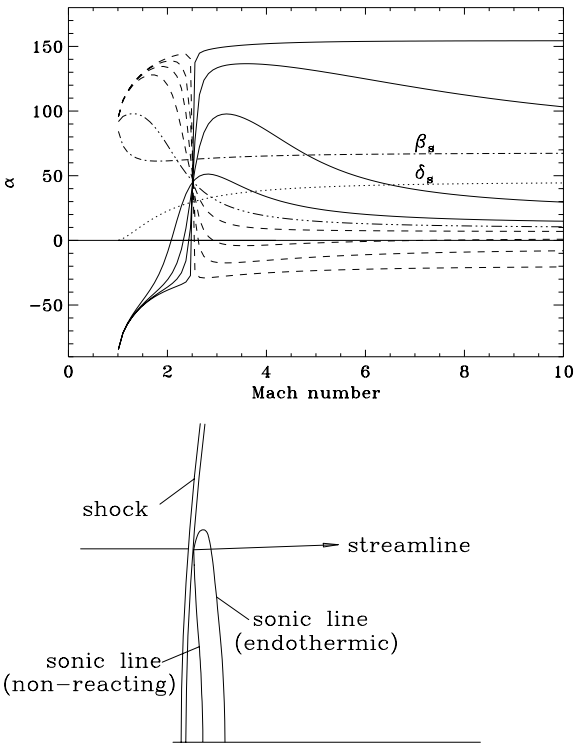

Fig. 13. *Top:* Dependence of sonic line angle on Mach number and reaction rate, plane flow, γ = 1.4, θ = 0.8. The deflection and shock angles at the sonic condition are also shown as a dotted and a chain–dotted line. The chain–dotted line with three dots is for the non–reacting case, in agreement with the solution given by Hayes and Probstein. Continuous lines and dashed lines represent endothermic and exothermic reaction rate cases respectively, for $k\varepsilon = -0.0001, -0.001, -0.003, -0.01, 0.01, 0.003, 0.001, 0.0001$. *Bottom:* Schematic sketch of shapes of subsonic pocket behind a plane convex shock in near–sonic flow

where $h_{\text{chem.}}$ is chemically stored specific energy and a is the frozen speed of sound. $V = a$ along the sonic line, for which we can therefore write

$$\frac{\gamma+1}{2(\gamma-1)}V^2 + h_{\text{chem.}} = h_0. \tag{60}$$

Differentiating this along the sonic line, and recalling that $c_{ix} = 0$,

$$V_x \cos\phi + V_y \sin\phi + \sin\phi \frac{\gamma-1}{\gamma+1}\frac{1}{V}\sum_{i=2}^{n} h_{c_i} c_{iy} = 0. \tag{61}$$

Here, ϕ is the angle between the sonic line and the shock. It is related to the angle α between the sonic line and the streamline through

$$\alpha = \phi - \beta + \delta,$$

see Fig. 12 for notation. Thus,

$$\tan\phi = \frac{-V_x}{V_y + \frac{\gamma-1}{\gamma+1}\frac{1}{V}\sum_{1=2}^{n} h_{c_i} c_{iy}}. \tag{62}$$

Figure 13 shows that, at high Mach number, endothermic reactions cause α to increase, and *vice versa*, but these trends are reversed at low Mach number. The reversal occurs at a particular Mach number, which, for the value of γ chosen,

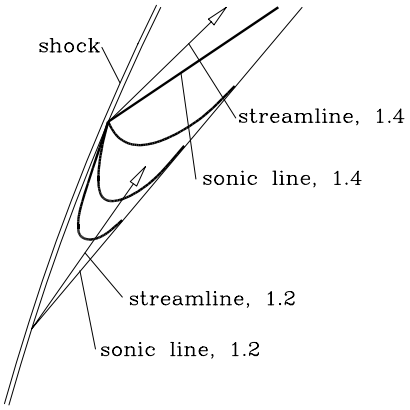

Fig. 14. Sketch of sonic lines for M = 10, γ = 1.4 with endothermic reaction. The equilibrium situation is modeled by a γ = 1.2 flow to provide the asymptotic sonic–line direction. The sonic lines for three reacting–flow cases and the frozen case are shown as heavy lines

is approximately 2.5. This is the point where the reaction rate term in V_y just cancels the one that occurs explicitly in the denominator of (62). This condition occurs at

$$\frac{p}{\rho v^2} = \frac{\gamma^2-\gamma+2}{\gamma^2-1}.$$

Using (8), (10) and (13) to express p, v and ρ in terms of M, γ and β then leads — for the particular value of $\beta = \beta_s(\gamma, M)$ at the sonic point — to a particular value of $M(\gamma)$ at which the reaction rate does not influence the sonic line slope.

For very fast reactions, ϕ switches from $-90°$ to +90° at this critical Mach number, so that, at large Mach number, the limiting sonic line direction for very fast reaction is along the shock. In endothermic flow it is at ϕ = +90° and in exothermic flow at $-90°$.

The response of the sonic line to reaction rate at high Mach number has been observed by Hornung and Smith (1979), who used it to make an argument about the influence of non–equilibrium dissociation on the shock detachment process in flow over a wedge. This behavior was also observed in recent numerical computations of these wedge flows by Candler (unpublished work). In endothermic flow near the shock, at high Mach number, streamlines cross the sonic line from a subsonic region, while, for sufficiently fast exothermic reactions, the opposite holds (negative α).

In the low Mach number range, the sonic line direction is very sensitive to slight heat removal by endothermic reaction. Near M = 1, a change from non–reacting to slow endothermic reaction switches α from +90° to $-90°$, while exothermic reactions have a weaker effect. This will cause the subsonic pocket behind a convex shock to change as shown in the sketch of Fig. 13. (bottom).

The effect of chemical reaction on the sonic line may be illustrated by considering frozen and equilibrium flow limits. In the endothermic case, the equilibrium limit is displaced, relative to the non–reacting limit, toward the direction of smaller γ. For smaller γ the sonic point is displaced to larger β. This is shown with the correct values of β_s in Fig. 14 for the example of a circular–arc shock at M = 10 with γ = 1.4 and 1.2. Also plotted are the correct streamline

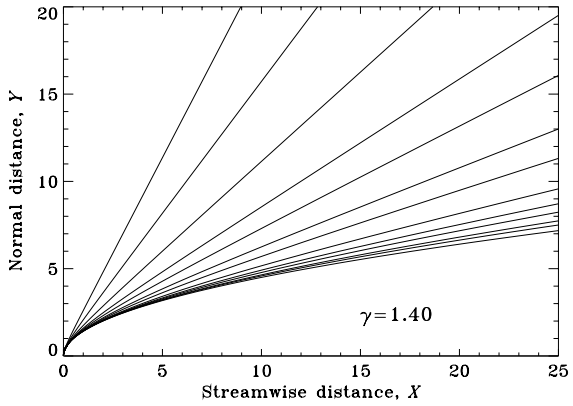

Fig. 15. Hyperbolic shock shapes, with finite curvature at the normal–shock point and asymptoting to a Mach wave at large X. Mach numbers are: 1.1, 1.2, 1.4, 1.7, 2, 2.5, 3, 4, 5, 6, 8, 10, 20

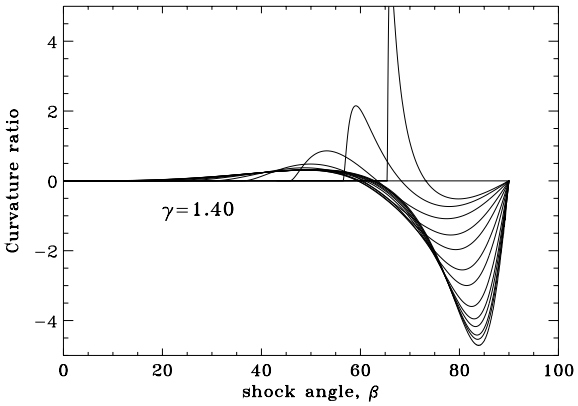

Fig. 16. Streamline–to–shock curvature ratio for axisymmetric shocks as shown in Fig. 15. Perfect gas, γ = 1.4, Mach numbers as in Fig.15. The ratio is the streamline curvature divided by the shock curvature k in the xy–plane

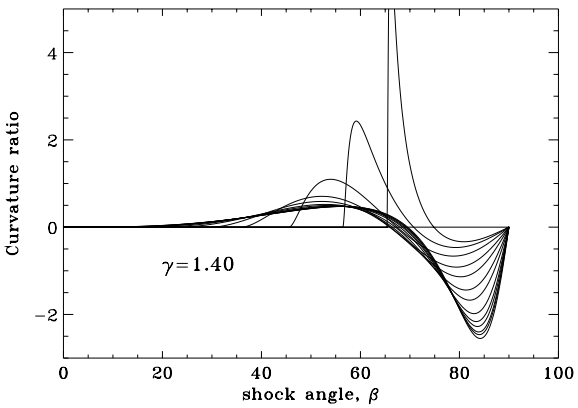

Fig. 17. Streamline–to–shock curvature ratio for plane shocks of the shape shown in Fig. 15. Perfect gas, γ = 1.4, Mach numbers as in Fig. 15

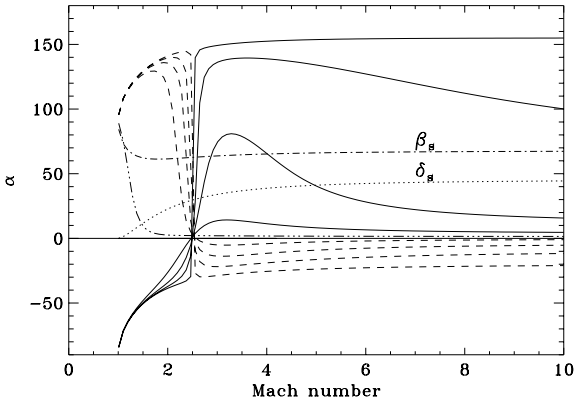

Fig. 18. Sonic line angle in axisymmetric flow. Shock shape as in Fig. 15, notation as in Fig.13. γ = 1.4, θ = 0.8, $k\varepsilon$ = $-0.0001, -0.001, -0.003, -0.01, 0.01, 0.003, 0.001, 0.0001$

and sonic line directions for the two cases. In flow with endothermic reaction, the sonic lines depart from the γ = 1.4 sonic point at angles α that increase with reaction rate. If the reaction is completed to equilibrium over a distance that is small compared with the shock radius of curvature, all the directions at equilibrium should be something like that for γ = 1.2 in this crude model. Thus, the sonic line for finite reaction rate leaves the γ = 1.4 sonic point at a finite angle relative to that of non–reacting flow and asymptotically blends into the γ = 1.2 sonic line. In the sketch, sonic lines for three finite rates are shown to illustrate how the transition from frozen flow to larger and larger rates proceeds.

The situation is reversed for exothermic flow. It is easily seen from Fig. 14 that the streamline always crosses the sonic line from the subsonic to the supersonic side with endothermic flow at these conditions, while both directions are possible with exothermic flow, as has been pointed out earlier.

8 Three–dimensional flows

Finally, consider the extension of these results to the more general case of three–dimensional flow. To this end, choose the $xy-$plane to be the plane of the free–stream direction and the local normal to the shock wave at the point of interest. With this choice, the velocity component in the third (z) direction and its gradients in the xy–plane are zero. Thus a suitable name for this plane is the "flow plane". By choosing x and y to lie in the flow plane, the derivatives of p, ρ and u with respect to z (the dimensionless coordinate normal to the flow plane) are zero, and the only non–zero gradient normal to the flow plane is

$$w_z = l,$$

where w is the dimensionless $z-$component of velocity and l is the shock curvature in the yz–plane. $k+l$ is the Gaussian curvature of the shock at the point considered.

If we write Eqs. (3 to 6) for y = 0, the only changes to these equations are that the term $-k\rho v$ in the continuity equation becomes $-(k+l)\rho v$, and a new term $-\rho l$ is added. The equation (at y = 0) becomes

$$(\rho u)_x - (k+l)\rho v + \rho l + (\rho v)_y = 0. \quad (63)$$

This causes additional terms proportional to l to appear in Eqs. (18), (20) and (21), for the y–derivatives of p, v, and ρ as follows:

$$p_y F = \ldots + l\rho h_\rho (1/v - 1), \quad (64)$$

$$v v_y F = \ldots + l\rho h_\rho (1/v - 1), \quad (65)$$

$$\rho_y F = \ldots + l(1 - 1/\rho + \rho/v). \quad (66)$$

Equation 19 for u_y remains unchanged.

A relatively simple example is that of axisymmetric flow. In this case, the flow plane is the meridional plane. Consider an axisymmetric shock wave of hyperbolic shape in the flow plane, such that the normal–shock point has finite curvature equal in both directions, and the shock is aymptotically conical with half–angle equal to the Mach angle far from this point. Defining the distance along the axis of symmetry, normalized by the radius of the shock at the nose, to be X, and the normal to it (similarly normalized) as Y, the shock shapes for a set of Mach number values are as shown in Fig. 15. The equation of the shock shape is

$$Y = \tan\mu \sqrt{X\left(X + \frac{2}{\tan^2\mu}\right)} \quad (67)$$

where μ is the Mach angle $\arcsin(1/M)$. This gives a shock angle β that can be determined from

$$\tan\beta = \frac{\tan\mu}{\sqrt{X}} \frac{1 + 1/(X\tan^2\mu)}{\sqrt{1 + 2/(X\tan^2\mu)}}. \quad (68)$$

Solving this for X,

$$X\tan^2\mu = \sqrt{\frac{\tan^2\beta}{\tan^2\beta - \tan^2\mu}} - 1. \quad (69)$$

With this, the shock curvature in the meridional plane becomes

$$k = (1 + 2X\cos^2\mu + X^2\sin^2\mu)^{-3/2}. \quad (70)$$

This gives an explicit relation between k and β with Mach number as a parameter. For an axisymmetric shock, the transverse curvature in the yz–plane is $l = \cos\beta/Y$. The shape of the shock now permits the streamline to shock curvature ratio to be determined for the axisymmetric and the plane case as functions of the shock angle β. The results are shown in Figures 16 and 17. These exhibit no qualitative differences. Quantitative changes include slight changes in the Crocco points and a greater negative value of the curvature ratio for axisymmetric flow.

It is interesting to find the effect of the third dimension on the sonic line slope at the shock. This is not new in non–reacting flow (see Hayes and Probstein), but our results permit it to be obtained directly for reacting flow also. Figure 18 shows how α behaves in an axisymmetric flow with the same shock shapes as in Fig. 15. The effect of reactions is very similar to that for plane flow.

Acknowledgements. Some of the work presented here has been part of various courses I have taught over the last 20 years at the Australian National University, at the University of Göttingen, and at Caltech. Many of my students have contributed in the form of discussions that have helped correct some mistakes. At Caltech, Professor J. E. Shepherd, in numerous discussions, contributed many ideas and important corrections, and he encouraged me to put this material together in a publication. My sincere thanks to them all.

References

Becker E (1972) Chemically reacting flows. Ann. Rev. Fluid Mech. 6:155

Clarke JF (1969) in Wegener PP: Non-equilibrium flows, Part II. Marcel Dekker

Hayes WD, Probstein RF(1959) Hypersonic Flow Theory. Academic press

Hornung HG (1976) Non–equilibrium ideal–gas dissociation after a curved shock wave. J. Fluid Mech. 74:143

Hornung HG, Smith GH (1979) The influence of relaxation on shock detachment. J. Fluid Mech. 3:225

Kewley DJ, Hornung HG (1974) Non–equilibrium nitrogen flow over a wedge 64:725

Lighthill MJ (1949) The flow behind a stationary shock. Phil. Mag. 40:214

Mölder S (1971) Reflection of curved shock waves in steady supersonic flow. CASI Trans. 40:73-80

Mölder S (1972) Polar streamline directions at the triple point of Mach interaction of shock waves. CASI Trans. 5:88-89

Munk MM, Prim RC (1948) Surface–pressure gradient and shock–front curvature at the edge of a plane ogive with attached shock front. J. aeron. Sci. 15:691

Oswatitsch K (1952) Gasdynamik. Springer